Analysis of the anisotropy decay of *trans*-parinaric acid in lipid bilayers

Anthony Ruggiero and Bruce Hudson
Department of Chemistry, Institute of Molecular Biology and Chemical Physics Institute, University of Oregon, Eugene, Oregon 97403

ABSTRACT An analysis is presented of the complex anisotropy behavior of *trans*-parinaric acid in single component DEPC lipid bilayers. It is shown that a model involving two species with distinct lifetime and motional behavior is required, and is adequate, to explain the observed data. In particular, the observed increase in the anisotropy at long times demonstrates the presence of a species with a long fluorescence lifetime that has a high anisotropy. The time dependence of the anisotropy for these two environments is treated using both a purely mathematical sum of exponentials and a constrained fit based on an approximate solution of the anisotropic diffusion problem. In this latter model the anisotropy is described in terms of the second and fourth rank order parameters, $\langle P_2 \rangle$ and $\langle P_4 \rangle$, and a single dynamical parameter, $D_\perp$, the perpendicular diffusion coefficient for this uniaxial probe. The parameters of both models are accurately determined from the fits to the data when two environments coexist and an association is made between lifetime components and distinct rotational sites. The values of the parameters obtained demonstrate the "solid-like" and "fluidlike" nature of these two coexisting environments.

INTRODUCTION

The time dependence of the emission anisotropy of fluorescent species in biopolymers or lipid bilayers is a useful way to determine the orientational order and dynamic mobility of these species (Kinosita et al., 1977, 1982; Kawato et al., 1977, 1978; Heyn, 1979; Jahnig, 1979*a* and *b*; Zannoni, 1981; Zannoni et al., 1983; Szabo, 1984; Ameloot et al., 1984; van der Meer et al., 1984). The asymptotic anisotropy observed at long times for a probe in a bilayer can be directly related to the second rank order parameter, $\langle P_2 \rangle$. The time dependence of the anisotropy at short times is related to the dynamic behavior of the emitting species. Fluorescence anisotropy measurements using modern methods permit the separation and measurement of the rate of internal motion as distinct from the amplitude of that motion. Because of the anisotropic nature of these systems, the connection between microscopic motional parameters and the observed time dependence of $r(t)$ requires applications of a model (Kinosita et al., 1977, 1982; Kawato et al., 1977, 1978), the use of approximate solutions of general cases (Zannoni, 1981; Zannoni et al., 1983; Szabo, 1984; Ameloot et al., 1984; van der Meer et al., 1984) or the use of molecular dynamics simulations (Northrup and Curvin, 1985; van der Ploeg and Berendsen, 1981; 1983; Busico and Vacatello, 1983; Kox et al., 1980).

The unique interpretation of anisotropy behavior is potentially complicated by the effects of heterogeneity of the population of fluorescent species. If all of the fluorophores of the sample have the same excited state decay behavior (the same lifetime in the simplest case), then the extracted motional and order parameters will be well-defined averages over the population. Similarly, if the population is homogeneous with respect to its motional and order behavior but is heterogeneous with respect to excited state decay behavior, then the values obtained from analysis of the anisotropy will again reflect the true dynamic properties. The complexity occurs when there is a correlation between the excited state decay and motional properties for subpopulations of the sample. Given the photophysical properties of many fluorophores, this is expected to be a common situation. In this case the time dependence of the anisotropy does not reflect motion *per se* because the anisotropy includes time-dependent weighting of the components of the population. For example, at long times the observed anisotropy is dominated by those species in the population with the longest lifetime. We have discussed this problem in qualitative terms and presented several experimental examples in previous work (Hudson et al., 1986, 1987). We have also presented the results of simulations showing the range of behavior that can be obtained in such cases (Ludescher et al., 1987). This phenomenon is well known in formal terms (Lakowicz, 1983; Dale et al., 1977; Claesens and Rigler, 1986; Rigler and Ehrenberg, 1973; Szabo, 1984) but there do not seem to be any examples where experiments exhibiting this effect have been subjected to an analysis resulting in decomposition of the overall anisotropy into the behavior of the individual environments. The successful demonstration of such a procedure, and the reliability of the resulting parameters, is one of the major points of this paper.

In the preceding article (Ruggiero and Hudson, 1989)

we demonstrated that at temperatures up to 15°C above the order-disorder phase transition there is a heterogeneity in single-component lipid bilayers that results in a nonexponential fluorescence decay for *trans*-parinaric acid. This behavior is attributed to critical fluctuations in these systems consistent with ultrasonic (Nagle, 1976; Doniach, 1978; Mitaku et al., 1978; Mitaku and Okano, 1981; Mitaku and Date, 1982; Mitaku et al., 1983) and ac calorimetry measurements (Hatta et al., 1983, 1984) and with theoretical arguments (Kanehisa and Tsong, 1978; Zuckermann and Pink, 1980; Jahnig, 1981*a–c*; Mouritsen et al., 1983; Mouritsen and Zuckerman, 1985). The ability to assign the components of the fluorescence decay of parinaric acid to environments with distinct density is based on the sensitivity of the fluorescence lifetime of this probe species to its environment (Sklar et al., 1977*a* and *b*). The known sensitivity of the absorption spectrum of parinaric acid to local density (Sklar et al., 1977*a* and *b*) was also utilized to characterize the individual probe environments in lipid bilayers (Ruggiero and Hudson, 1989). There is a strong correlation between density and acyl chain order in lipid bilayers. Because of this, and because of the fact that *trans*-parinaric acid has a fluorescence lifetime that depends on density, it is expected and observed that the anisotropy of the fluorescence of *trans*-parinaric acid will exhibit anomalous behavior in bilayer systems in the temperature range where two distinct environments coexist. In the present work we show that the order parameters and rotational diffusion coefficients extracted from a heterogeneous model of the lipid bilayer are consistent with the interpretation of coexisting domains that have "solidlike" and "fluidlike" properties. The quantitative variation of these dynamic properties is discussed.

MATERIALS AND METHODS

The fluorescent species used in this study is *trans*-parinaric acid, a well-characterized fluorescent probe (Sklar et al., 1975, 1976, 1977*a* and *b*; Wolber and Hudson, 1981, 1982; Hudson et al., 1986, 1987; Hudson and Cavalier, 1987). The major features of this species used in the present application are the collinearity of its absorption and emission transition dipoles and the fact that the fluorescence lifetime of parinaric acid is a sensitive function of its environment. Specifically, the lifetime is much longer in environments with a high density than for those with a low density. This results in a large decrease in the fluorescence lifetime for this probe in a lipid bilayer when the temperature is increased through T_m, the temperature of the order-disorder phase transition. Lipid vesicles were prepared using the injection method of Kremer et al. (1977) as previously described (Ruggiero and Hudson, 1989). Anisotropy and total intensity decay measurements were made by time-correlated single photon counting (Fleming, 1986) with a picosecond dye laser-based system and a microchannel plate detector. The intrinsic time resolution of the instrument (full width at half height of the response function) is on the order of 150 ps. The experimental aspects of this study are described in some detail in the previous paper (Ruggiero and Hudson, 1989).

METHODS OF DATA ANALYSIS

Fluorescence lifetime data obtained with "magic angle" polarization were analyzed using both the method of moments (Isenberg and Dysan, 1969) with moment index displacement (Isenberg, 1973; Small and Isenberg, 1977) and by iterative reconvolution using a Marquardt nonlinear least squares algorithm (Marquardt, 1963). The quality of the fits obtained with the nonlinear least squares fitting procedures were judged by the (reduced) χ^2 value and the randomness of the modified residuals (residuals divided by the square root of the number of counts). "Randomness" of the deviation between the calculated and observed data was evaluated by visual inspection of plots of both the residuals and the Poisson weighted autocorrelation function of the residuals versus channel number and also by the "runs test" (time sequence of signs + or −) of the residuals (Ameloot and Hendrickx, 1982; Grinvald and Steinberg, 1974). The quality of the method of moments analyses was determined by the agreement between results obtained at different moment displacement values, the lambda-invariance test based on exponential depression, and component incrementation (Isenberg and Small, 1982; Libertini and Small, 1983). In both methods the total fluorescence intensity was assumed to decay as a sum of exponentials.

The anisotropy data were fit using a Marquardt nonlinear least squares search. The horizontal and vertical fluorescence decay curves were simultaneously fit (Fleming and Cross, 1984) using separate horizontal and vertical response functions determined at the same count rate as their corresponding fluorescence decay components. The anisotropy data were fit to four different models as follows.

The first model, designated r_e, is an unconstrained sum of exponentials, a purely mathematical fit to the data. If rotational homogeneity of the sample is assumed, this model has the form:

$$r_e(t) = \sum_{j=1}^{m} b_j \exp(-t/\phi_j) + b_{m+1}, \quad (1)$$

where $r(\infty) = b_{m+1}$ is the anisotropy at long time. The number of exponential terms, m, is two or three as discussed below. The fundamental anisotropy at time $t = 0$ is given by

$$r_e(0) = \sum_{j=1}^{m+1} b_j \quad (2)$$

Heterogeneity of the bilayer in terms of the correlated

variation of the fluorescence decay and anisotropy behavior is accounted for by an "associated" exponential model of this type, designated r_{ac}, in which the lifetime and amplitude of the total intensity decay components are now specifically associated with individual anisotropy parameters

$$r_{ac}(t) = \sum_{i=1}^{n} f_i(t) r_i(t), \tag{3}$$

where

$$f_i(t) = a_i \exp(-t/\tau_i)/I_T(t), \tag{4}$$

$$I_T(t) = \sum_{i=1}^{n} a_i \exp(-t/\tau_i) \tag{5}$$

and

$$r_i(t) = \sum_{j=1}^{m_i} b_{ij} \exp(-t/\phi_{ij}) + b_{i,m+1}. \tag{6}$$

The number of environments, n, is two for the cases analyzed here. The amplitudes associated with each environment, a_i, are determined from an analysis of the total fluorescence decay. In the case of parinaric acid in hydrocarbon solution and in fluid bilayer environments, the fluorescence decay appears to require two exponential terms for an adequate description. In such cases the weighting factor f_i consists of a sum of two exponential terms. The number of terms describing the decay of the anisotropy in the ith environment, m_i, is set equal to one for the analyses presented here. Each environment is characterized by a specific limiting anisotropy, rotational diffusion coefficient and second and fourth rank order parameters.

In either of these models the perpendicular diffusion coefficient is given by

$$D_{\perp i} = \left(\frac{1}{6}\right) r(0) \sum_{j=1}^{m} b_{ij}/\phi_{ij}, \tag{7}$$

and the second rank order parameter is given by

$$\langle P_2 \rangle = [r(\infty)/r(0)]^{1/2}. \tag{8}$$

The other pair of analyses are based on the model of van der Meer et al. (1985) resulting from an approximate solution of Smoluchowski equation (van der Meer et al., 1984; Szabo, 1984). This "constrained" model in its "unassociated" form is designated r_c. In this model the anisotropy is expressed in terms of the perpendicular diffusion coefficient $D_\perp$ and the order parameters $\langle P_2 \rangle$ and $\langle P_4 \rangle$. The expression for this constrained model r_c is

$$r_c(t) = \sum_{j=1}^{3} b_j \exp(-t/\phi_j) + b_4, \tag{9}$$

where the b_j and ϕ_j are functions of $D_\perp$, $\langle P_2 \rangle$, and $\langle P_4 \rangle$ as given in Table 1. (The expression for ϕ_2 given in Ameloot et al., 1984, Table 3, has been corrected by inclusion of a factor of 2.)

The corresponding heterogeneous version of the van der Meer model with inclusion of associated fluorescence decay and rotational motion is given by

$$r_{ac}(t) = \sum_{i=1}^{n} f_i(t) r_{ic}(t), \tag{10}$$

where $f_i(t)$ is given by Eq. 4, $r_{ic}(t)$ is given by Eq. 9 and Table 1, and $I(t)$ is given by Eq. 5.

Elaborate descriptions of the time-dependent anisotropy that allow all parameters to be freely adjustable may result in large uncertainties for the estimated parameters. To reduce the number of free parameters, the initial anisotropy at time $t = 0$, r_0, known as the fundamental anisotropy, is usually fixed at a predetermined value in the analysis (Ameloot et al., 1984; Kinosita et al., 1982). The logical choice for this value is the theoretical limit determined by the relative orientations of the absorption and emission dipoles, or the experimentally determined value from a steady-state measurement of the probe under completely rigid conditions. Unfortunately, in situations involving complex decays, instrumental time resolution often plays an important role in determining the observed value of r_0. Motions too fast to be resolved will appear as instantaneous rotations of the transition dipoles and result in the lowering of r_0 from the theoretical value (Szabo, 1984; Zinsli, 1977). In these cases, fixing r_0 at the theoretical limit or at a value determined under conditions where these fast librational motions may not be present may result in poor quality fits or in distortions of

TABLE 1 Expressions for the decay of the anisotropy of a uniaxial fluorescence probe with a distribution function characterized by $\langle P_2 \rangle$ and $\langle P_4 \rangle$

$$r(t) = \sum_{j=1}^{3} b_j \exp(-t/\phi_j) + r_0 \langle P_2 \rangle^2$$

j	b_j	ϕ_j
1	$r_0(1/5 + 2\langle P_2 \rangle/7 + 18\langle P_4 \rangle - \langle P_2 \rangle^2)$	$b_1/6r_0D_\perp(1/5 + \langle P_2 \rangle/7 - 12\langle P_4 \rangle/35)$
2	$2r_0(1/5 + \langle P_2 \rangle/7 + 3\langle P_4 \rangle/35)$	$b_2/12r_0D_\perp(1/5 + \langle P_2 \rangle/14 + 8\langle P_4 \rangle/35)$
3	$2r_0(1/5 - 3\langle P_2 \rangle/7 + 3\langle P_4 \rangle/35)$	$b_3/12r_0D_\perp(1/5 - \langle P_2 \rangle/7 - 2\langle P_4 \rangle/35)$

the estimated parameters. The procedure used in this work involved first analyzing the data with all parameters freely adjustable and then reanalyzing the data with r_0 fixed at the value obtained from the free fit. To determine the effect of r_0 on the estimated parameters, additional analyses were performed with r_0 fixed at several different values. In all cases, the fits were of poorer quality and the estimated parameters had larger uncertainties than when r_0 was fixed at the free fit value. Although the actual parameter values and fit quality varied at different fixed values of r_0, the estimated parameters always showed the same qualitative behavior.

The recovered parameters were independent of fitting range within the statistical and experimental error of the measurement, but the quality of the fits were often poorer ($\chi^2 \approx 1.5$ rather than 1.0–1.2) when the rising edge of the response function was included in the analysis. Because the fluorescence lifetime parameters in an anisotropy experiment are usually calculated from the horizontal and vertical polarization decay components, comparison of these values with the total fluorescence decay measured under the same conditions but at the magic angle provides a good internal consistency check of the data quality. In all cases the fluorescence decay parameters calculated from the fluorescence polarization decay components of the anisotropy experiments were in good agreement for different anisotropy models and with the magic angle lifetime data.

RESULTS

The time dependence of the fluorescence anisotropy of *trans*-parinaric acid in a bilayer composed of dielaidoylphosphatidylcholine (DEPC) at 17°C is shown in Fig. 1. The corresponding behavior at other temperatures is presented in Figure 7 of Ruggiero and Hudson, 1989 (see also Hudson et al., 1986, Fig. 8, and Hudson et al., 1987, Fig. 2). The major point of interest is the increase in the anisotropy at long times for some temperature values. This behavior, in conjunction with the large value of r_0, is inconsistent with any homogeneous model for the fluorophore environment (Ludescher et al., 1987; Hudson et al., 1987). The analysis of such results in terms of the models presented above is the main objective of the present work. The parameter values resulting from such an analysis are given in Table 2 and presented in Figs. 2 and 3. Fig. 1 shows the optimized fit of the r_{ae} model to the data at 17° and includes plots of the modified residuals for this fit for the individual parallel and perpendicular transients. It is clear that this model gives an excellent fit to the data.

Within a given analysis classification (i.e., associated or nonassociated), the unconstrained mathematical models (r_e and r_{ae}) and the constrained models (r_c and r_{ac}) gave equally good statistical fits. In the constrained models, the anisotropy decay is described as the sum of three exponential terms plus a constant. The parameters of the decay are determined by $\langle P_2 \rangle$, $\langle P_4 \rangle$, and $D_\perp$. In all

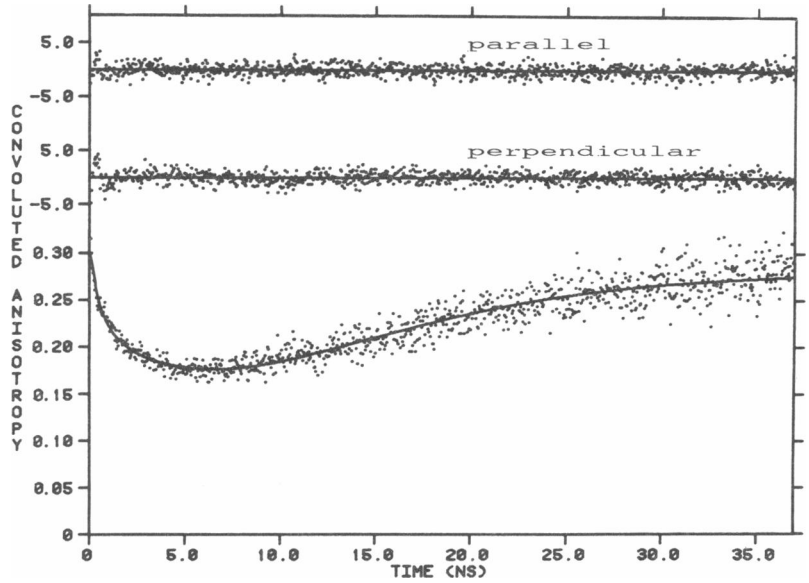

FIGURE 1 The time-dependent anisotropy decay of *trans*-parinaric acid in dielaidoylphosphatidyl choline vesicles at 17°C. The points are data; smooth curves represent the appropriately convoluted optimized fit to the data using the associated exponential model. The curves at the top are plots of the modified residuals for the parallel and perpendicular transients, i.e., the difference between the calculated and observed values divided by the square root of the observed value.

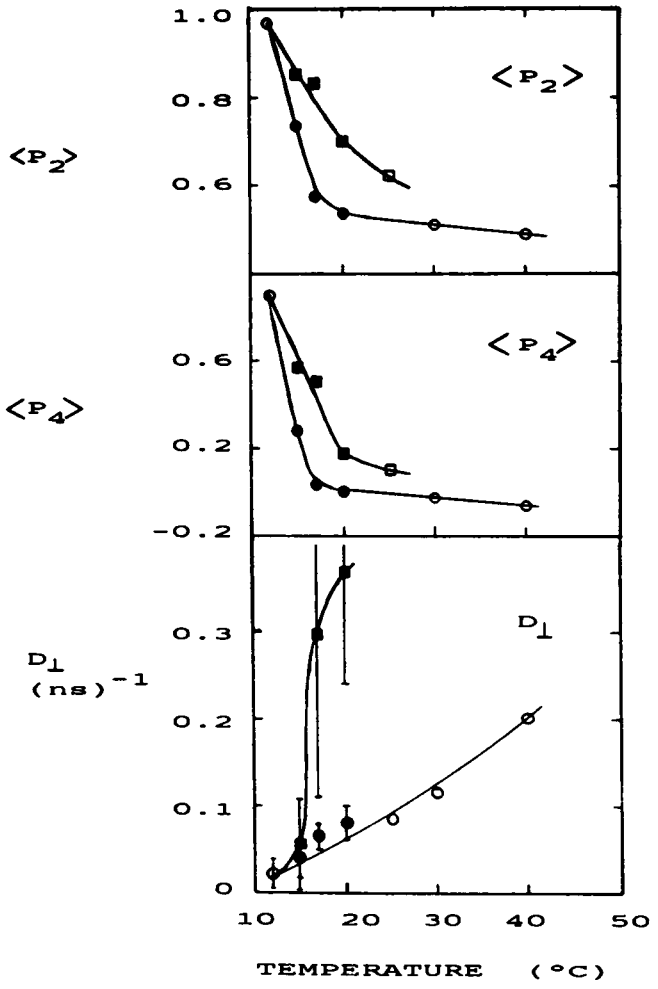

FIGURE 2 Temperature dependence of the second and fourth rank order parameters and the perpendicular diffusion coefficient of *trans*-parinaric acid in DEPC bilayers. (*Circles*) Fluid (short lifetime) environment; (*squares*) solidlike (long lifetime) environment. Solid symbols are from fits to the data of associated anisotropy models that assume rotational heterogeneity. Open symbols are from fits to the data that assume rotational homogeneity. In the $\langle P_2 \rangle$ plot the largest statistical error is slightly smaller than the symbols; in the $\langle P_4 \rangle$ plot the largest statistical error is slightly larger than the symbols. The statistical error limits are shown in the $D_\perp$ plot unless they are smaller than the symbols.

models, the long-time asymptotic value of the anisotropy is given by $r_0\langle P_2 \rangle^2$. Although the constrained models contain more exponential terms, the actual number of adjustable parameters is less than in an unconstrained fit to a sum of two exponentials because all the correlation times and preexponential factors are functions of only the three parameters $\langle P_2 \rangle$, $\langle P_4 \rangle$, and $D_\perp$. The two-exponential mathematical models contain four adjustable parameters. Furthermore, the constrained models permit an estimation of the higher order orientational order parameter $\langle P_4 \rangle$. It is interesting to note that when a free-floating unconstrained exponential model is used the anisotropy data is best fit by a model that contains only two exponentials and a constant. Attempts to fit the data with three unconstrained exponentials resulted in two identical correlation times and very large uncertainties in the estimated parameters due to cross-correlation. This seems to suggest the need for a constrained model when fitting complex anisotropy data with multiple exponential models.

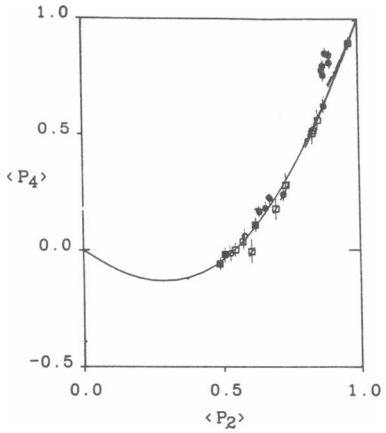

FIGURE 3 The variation of $\langle P_4 \rangle$ with $\langle P_2 \rangle$ for *trans*-parinaric acid in DEPC vesicles (solid and open squares corresponding to anisotropy models assuming rotational homogeneity and heterogeneity, respectively) and for cholesterol/DEPC mixtures (*solid circles*). Open circles represent results for the analysis of *trans*-parinaric acid in DPPC bilayers analyzed on the basis of a homogeneous model (Ruggiero, 1986). The smooth curve shows the relationship between $\langle P_4 \rangle$ and $\langle P_2 \rangle$ for the rotational diffusion within a cone model (Kinosita, et al., 1977; van der Meer, 1984).

In all of the models, the value of the fundamental anisotropy, r_0, in the bulk fluid phase lipids is found to be significantly lower than that observed in either the solidlike lipid clusters near the transition point or in solid phase lipids for temperatures well below the order-disorder transition temperature. In principle, the value of r_0 should depend only on the relative orientations of the absorption and emission transition dipoles. The theoretical value of r_0 for a molecule with parallel transition dipole moments is 0.4. The experimentally determined value of r_0 in solid-phase lipids and the solidlike lipid clusters in the fluid phase is 0.38–0.4. In the fluid phase bilayer a value of r_0 near 0.3 is obtained from the data. A value of r_0 that is lower than the theoretical maximum can result either from an "instantaneous" rotation of the transition dipoles due to electronic relaxation or from molecular motions that are too rapid to be experimentally resolved. The fact that values of r_0 close to the theoretical

TABLE 2 Parameter values resulting from analysis of the anisotropy decay of *trans*-parinaric acid in DEPC bilayers

		Exponential Analysis									
EX	T	a_1	$R_0(1)$	$R(1)$	$\phi(1)$	$\frac{C(1)}{[\langle P_2(1)\rangle]}$	$R_0(2)$	$R(2)$	$\phi(2)$	$\frac{C(2)}{[\langle P_2(2)\rangle]}$	χ^2
300	12	0.829 (0.006)	0.333	0.021 (0.00)	0.467 (0.049)	0.312 [0.968]		0.0 (0.0)	1.0 (0.0)		1.15
300	15	0.243 (0.032)	0.397	0.105 (0.002)	0.893 (0.177)	0.292 [0.858]	0.298	0.130 (0.007)	2.612 (0.286)	0.159 [0.730]	1.08
300	17	0.173 (0.004)	0.400	0.124 (0.001)	0.202 (0.047)	0.276 [0.831]	0.280	0.180 (0.002)	2.186 (0.055)	0.100 [0.598]	1.19
320	17	0.169 (0.008)	0.397	0.118 (0.001)	0.285 (0.060)	0.279 [0.838]	0.289	0.179 (0.003)	2.214 (0.063)	0.110 [0.617]	1.46
300	20	0.065 (0.003)	0.380	0.195 (0.003)	0.299 (0.096)	0.185 [0.698]	0.279	0.189 (0.001)	1.954 (0.027)	0.090 [0.568]	1.31
320	20	0.075 (0.004)	0.400	0.187 (0.005)	0.286 (0.234)	0.213 [0.730]	0.323	0.221 (0.001)	1.539 (0.021)	0.102 [0.562]	1.49
300	25	0.042 (0.007)	0.318	0.116 (0.004)	2.757 (0.097)	0.120 [0.614]		0.082 (0.005)	0.687 (0.029)		1.25
300	30	0.015 (0.002)	0.297	0.110 (0.015)	2.441 (0.261)	0.073 [0.496]		0.114 (0.015)	0.695 (0.080)		1.33
300	40	0.013 (0.001)	0.314	0.156 (0.005)	1.250 (0.039)	0.071 [0.476]		0.087 (0.006)	0.288 (0.018)		1.25
320	40	0.014 (0.001)	0.322	0.156 (0.003)	1.367 (0.033)	0.071 [0.470]		0.095 (0.004)	0.265 (0.012)		1.10

Relaxation times are given in nanoseconds, diffusion coefficients in reciprocal nanoseconds. Estimates of the statistical uncertainty are given in parentheses. a_1 is the amplitude of the long-lifetime fluorescence component. For both the exponential analysis (*left*) and constrained analysis (*right*), an associated model (r_{ae} or r_{ac}, respectively) was applied to the data obtained at 15–20°. For lower and higher temperatures a homogeneous model was found to be adequate to fit the data. For the homogeneous fit there is a single value of r_0; there are two exponential components for the anisotropy decay. In these cases $R(i) = b_i$ and $C(1) = b_3$ as used in Eq. 1. In the associated models the labels 1 and 2 refer to the two environments with their

maximum are observed in solid-phase lipids suggests that the lower value in the fluid phase bilayer is due to a motional component that is too fast to be detected under the present experimental conditions. The depolarization mechanism must be faster than 100 ps and must change the angle between the absorption and emission dipoles by ~24° to result in a lowering of r_0 to a value on the order of 0.3. Isomerization of the all-*trans* tetraene chromophore to a *cis* isomer might occur on this timescale (Granville et al., 1980) but this is only expected to change the transition dipole orientations by a small amount if at all. The most probable candidates for the depolarization mechanism are *trans-gauche* isomerizations in the saturated part of the *trans*-parinaric acid that induce rapid librations of the chromophore or rigid body tilting of the entire molecule. Concerted *trans-gauche* excitations (kink formation) would not depolarize the emission because this motion does not reorient the transition dipole. The possibility that this rapid depolarization of the emission may be due to rigid body tilting of the molecules is consistent with recent molecular dynamics simulations of lipid bilayers and monolayers (Northrup and Curvin, 1985; van der Ploeg and Berendsen, 1981, 1983). These calculations result in a cooperative rigid body tilting of the lipid hydrocarbon chains on the 10–20–ps timescale with a tilt angle on the order of 10–30° (van der Ploeg and Berendson, 1981). Cooperative tilting of the lipid acyl chains has been proposed as a "gating" mechanism that modulates the nucleation of disordered lipid domains in the phase transition region (Northrup and Curvin, 1985). The determination of the exact nature of the fluorescence depolarization mechanism giving rise to the low r_0s found in fluid-phase lipid bilayers requires further experimental investigation. One approach is the use of analogues of parinaric acid with the conjugated tetraene moved to another position in the acyl chain because this changes the possibilities for *trans-gauche* isomerization.

A comparison of the limiting anisotropy and rotational diffusion coefficients obtained from the constrained and unconstrained models (Table 2) is useful because it gives

Constrained Analysis										
$R_0(1)$	$\langle P_2(1)\rangle$	$\langle P_4(1)\rangle$	$D^c_\parallel(1)$	$D^c_\perp(1)$	$R_0(2)$	$\langle P_2(2)\rangle$	$\langle P_4(2\rangle$	$D^c_\parallel(2)$	$D^c_\perp(2)$	χ^2
0.333	0.968 (0.001)	0.896 (0.034)	0.022 (0.017)	0.022 (0.005)						1.12
0.397	0.857 (0.003)	0.564 (0.059)	0.055 (0.058)	0.049 (0.187)	0.288	0.739 (0.018)	0.282 (0.068)	0.039 (0.022)	0.027 (0.176)	1.03
0.397	0.836 (0.002)	0.505 (0.005)	0.294 (0.191)	0.255 (0.100)	0.285	0.576 (0.010)	0.038 (0.072)	0.063 (0.014)	0.049 (0.031)	1.16
0.397	0.840 (0.002)	0.517 (0.046)	0.352 (0.227)	0.173 (0.109)	0.306	0.609 (0.008)	−0.004 (0.034)	0.095 (0.012)	0.046 (0.042)	1.45
0.390	0.702 (0.006)	0.180 (0.074)	0.364 (0.124)	0.286 (0.173)	0.286	0.548 (0.005)	0.003 (0.085)	0.080 (0.021)	0.057 (0.019)	1.23
0.385	0.748 (0.008)	0.284 (0.020)	0.316 (0.283)	0.272 (0.435)	0.333	0.544 (0.003)	0.037 (0.048)	0.095 (0.012)	0.074 (0.017)	1.37
0.318	0.624 (0.001)	0.111 (0.022)	0.081 (0.005)	0.084 (0.004)						1.44
0.294	0.508 (0.002)	−0.017 (0.015)	0.116 (0.004)	0.117 (0.031)						1.35
0.306	0.488 (0.002)	−0.058 (0.016)	0.202 (0.008)	0.226 (0.002)						1.28
0.309	0.489 (0.002)	−0.065 (0.020)	0.200 (0.010)	0.244 (0.003)						1.15

distinct parameter values. The limiting anisotropy values $C(1)$ and $C(2)$ have been converted to the corresponding values of $\langle P_2\rangle$ using Eq. 8 and are given in square brackets in columns 7 and 11 for comparison with the results of the constrained analysis given in columns 14 and 19. Similarly, the values of $D_\perp$ obtained from the mathematical exponential analysis using Eq. 7 are given in columns 17 and 22 (labeled $D^c_\perp[1]$ and $D^c_\perp[2]$) for comparison with the values obtained directly from the constrained analysis ($D^c_\perp[1]$ and $D^c_\perp[2]$) given in columns 16 and 21.

an indication of the reliability of the estimated value of $\langle P_4\rangle$. The limiting anisotropy is model-independent, although its actual value depends slightly on the specific expression used in the fitting procedure because of correlations with the other parameters. The values obtained for the different models are almost identical. The rotational diffusion coefficients obtained from both types of models are also in reasonable agreement. This is significant because in the constrained models the rotational diffusion coefficient and $\langle P_4\rangle$ are correlated, while in the unconstrained models the diffusion coefficient is calculated from the preexponential factors and correlation times. The larger uncertainties for the rotational diffusion coefficients of the solid-phase environment compared with those for the coexisting fluid phase obtained from the lifetime-associated models can be attributed to a lack of precision in the data due to the relatively small amplitude of the long-lifetime component. The similarity in magnitude of the rotational correlation time associated with the long-lifetime species to the instrument response function width also aggravates the deconvolution problem for this complex analysis and makes it difficult to determine this parameter with precision.

It is not possible to obtain an adequate fit to the anisotropy decays that exhibit upward curvature without assuming rotational heterogeneity with association of the fluorescence lifetime components and the anisotropy decay behavior. This is described more generally elsewhere (Ludescher et al., 1987). Furthermore, excellent fits to the data are obtained using an associated model involving only two probe environments. This demonstrates that such a simple model is adequate for this anisotropy data in agreement with the treatment of the total fluorescence decay data presented previously (Ruggiero and Hudson, 1989). The temperature dependence of the order parameters $\langle P_2\rangle$, $\langle P_4\rangle$, and $D_\perp$ determined from the constrained models for DEPC above the phase transition temperature is shown in Fig. 2. These plots contain the results for each of the two environments in those cases where an associated model is required and the

values obtained from a nonassociated fit when that was adequate. The variation of $\langle P_4 \rangle$ with $\langle P_2 \rangle$ is presented in Fig. 3. These figures demonstrate the general precision of the data because the resulting plots show smooth variation of these derived parameters.

DISCUSSION

The most important result of the analysis of the complex anisotropy data of *trans*-parinaric acid in DEPC bilayers is that the resulting order parameters supports the view that the long-lifetime component of the fluorescence decay is associated with an environment having $\langle P_2 \rangle$ and $\langle P_4 \rangle$ values that are consistent with a solidlike environment. The values of $\langle P_2 \rangle$ for the environment associated with the long lifetime is consistently higher than that of the coexisting fluid phase at the same temperature. This is, in a sense, a necessary consequence of the upward curvature of the anisotropy decays at long times. The fact that the $\langle P_4 \rangle$ values are also higher for the solid environment than for the fluid environment is not obvious from the behavior of the anisotropy decays but is revealed by the detailed data analysis.

The temperature variation of $\langle P_2 \rangle$ and $\langle P_4 \rangle$ for the solidlike clusters and the fluid phase (Fig. 2, *a* and *b*) show distinct behavior. These order parameters for the fluid phase show a sharp, nearly discontinuous change as the phase transition temperature is approached. The corresponding solid-phase parameters show a smooth variation over a wider temperature range. The distinct behavior of the two components indicates that the phase transition has been resolved into a first-order transition undergone by the bulk fluid-phase lipids and a continuous second-order transition undergone by the solidlike clusters. Microscopically this can be understood by the fact that molecules in bulk fluid phase can cooperatively interact, whereas the interaction between lipid clusters in the transition region is screened by a boundary layer of lipids in intermediate states. The existence of a boundary layer within which the value of the order parameter varies continuously from that inside the cluster to that of the surrounding disordered bulk lipid is essential because the formation of a cluster with a sharp boundary would be energetically unfavorable. The fourth rank order parameter exhibits similar behavior to the second rank order parameter. This behavior is also reflected in the variation of the amplitudes of the fluorescence lifetime components as discussed previously (Ruggiero and Hudson, 1989).

Excitation of *trans*-parinaric acid fluorescence at 320 nm, near the "red edge" of its absorption, results in an increased amplitude for the solid-phase component of the fluorescence decay (Ruggiero and Hudson, 1989). This is due to the higher density and increased polarizability of this environment (Sklar et al., 1977*a* and *b*). Variation of the excitation wavelength from 300 to 320 nm also yields higher values for the order parameters in both the lifetime-associated and -unassociated models for temperatures near the phase transition point (Table 2). This suggests that either solidlike clusters of slightly different densities are being sampled or different regions of the clusters are being sampled. The center of a cluster, for example, is expected to be denser and have a higher order parameter than the edge. This suggests that a model with a distribution of environments may be needed to explain the data in complete detail.

The smooth variation of the extracted diffusion coefficient $D_\perp$ as a function of temperature (Fig. 2 *c*) demonstrates the statistical reliability of these values and the reproducibility of the experiments. Similar values are obtained for 300 and 320 nm excitation despite the variation in the value of $\langle P_2 \rangle$ with excitation wavelength discussed above.

An important conclusion from the data presented in Table 2 and Fig. 2 is that the rotational diffusion coefficient obtained for the solidlike clusters is much larger than that obtained for the actual solid phase at 12°C and also much larger than that for the surrounding fluid lipid at the same temperature. This behavior can be rationalized in terms of the Dissado and Hill model for the formation and regression of structural fluctuations (Dissado and Hill, 1983, 1982; Dissado, 1984; Dissado et al., 1985). In this model, the excess energy of the fluctuation, which is stored as local mechanical strain in the cluster at the time of its creation, is converted into the kinetic energy of local displacement motions. The excess local heat content of the cluster is removed as it regresses by dissipation into the many degrees of freedom of the surrounding disordered "bath" via regionalized lattice modes (phonons). The much larger rotational diffusion coefficients observed for the solidlike lipid clusters reflects the excess kinetic energy of the clusters relative to the bulk fluid-phase lipids. The conversion of the initial potential energy of the cluster into the molecular rotational motion of the constituent lipids seems reasonable because the excitation of intramolecular vibrations would require much more energy and *trans-gauche* excitations would result in the destruction of the cluster.

Another noteworthy feature of the data in Fig. 2 *c* is the rapid decrease in value of the rotational diffusion coefficient (increase of the rotational correlation time) of the probe in both the bulk fluid phase and solidlike clusters as the transition temperature is approached. It is tempting to attribute the slowing down of the reorientational motion of the probe in the bulk fluid phase with an increase in cooperative molecular interactions as the transition point is approached. An examination of the rotational diffusion coefficient simply as a function of the

order parameter from different lipid samples, however, reveals that the value of the diffusion coefficient is also strongly correlated with the order of the bilayer regardless of the distance from the transition point. The nonlinear relationship between the bilayer order and the rotational diffusion coefficient suggests that a simple hydrodynamic description of fluid probe interactions in the bilayer may not be appropriate. It should be noted that whereas the lower value of r_0 and the inability to resolve a very fast component in the fluid-phase bilayer anisotropy decay will certainly affect the accuracy of the recovered value of the diffusion coefficient, the magnitude of the trends observed here are much too large to be attributed solely to this type of fitting artifact.

Hydrodynamic theories generally predict a linear dependence of the rotational diffusion coefficient on temperature and viscosity unless either the coupling between the molecule and the bulk is temperature dependent (Kowert and Kivelson, 1976) or there is a turnover between slip and stick boundary conditions as the density increases (Hynes et al., 1978). In general, molecular rotation in a dense fluid is influenced by both microscopic and collective (hydrodynamic) effects (Hynes et al., 1978). The relative contributions of these two effects on molecular rotational and orientational motion in liquids has been discussed in great detail (Hynes, 1977). In cases such as this where the probe molecules and the molecules which make up the surrounding fluid are the same size, microscopic collisional effects are expected to dominate. It is quite possible that for *trans*-parinaric acid in lipid bilayers near the transition point several complex microscopic and collective interactions occur and are coupled.

The constrained r_c and r_{ca} descriptions of the fluorescence anisotropy are completely general in the sense that they represent approximate solutions of the Smoluchowski diffusion equation that have been obtained without specifying beforehand the type of uniaxial potential in which the probe molecules move. Because the anisotropy decay in these models gives information on the two parameters, $\langle P_2 \rangle$ and $\langle P_4 \rangle$, the acyl chain order information at a particular temperature can be conveniently represented as a point in a $\langle P_2 \rangle$, $\langle P_4 \rangle$ plane (van der Meer et al., 1984). The models for rotational diffusion on a cone (Wolber, 1980) and within a cone (Kinosita, 1977) as well as the Gaussian or Maier-Saupe model in which the reorientational potential appearing in the Smoluchowski equation is taken proportional to $P_2(\cos\theta)$ are all completely characterized by $\langle P_2 \rangle$ because $\langle P_4 \rangle$ is a specified function of $\langle P_2 \rangle$ for each model. The characteristic $\langle P_2 \rangle / \langle P_4 \rangle$ relationships for the specific models that have been proposed for the motion and distribution of acyl chains in bilayers can then be compared with the experimental data. Such a comparison of the DEPC data obtained here with the simple "diffusion in a cone" model (Kinosita, 1977) is presented in Fig. 3. The good agreement between the data obtained under conditions where two rotationally distinct environments were assumed (i.e., near the phase transition point) and the data obtained far from the transition point where rotational homogeneity was assumed demonstrates that the overall approach used to analyze the data is internally consistent and at least qualitatively correct. It is also of interest that this $\langle P_2 \rangle / \langle P_4 \rangle$ correlation obtained for *trans*-parinaric acid is quite different from that obtained for diphenylhexatriene (Ameloot et al., 1984). A more detailed discussion of this and other data, comparisons with other models and the interpretation of the angular distribution functions in terms of information theory is presented in another publication (Ruggiero and Hudson, manuscript in preparation). The main point here is that the complex, often rising, anisotropy behavior observed for *trans*-parinaric acid in a single component lipid bilayer can be interpreted in terms of a two-domain model consistent with critical behavior (Ruggiero and Hudson, 1989), a reasonable acyl chain angular distribution function and a smooth variation of the perpendicular diffusion coefficient with temperature.

This work was supported by National Institutes of Health grant GM26536.

Received for publication 28 October 1988.

REFERENCES

Ameloot, A., and H. Hendrickx. 1982. Criteria for model evaluation in the case of deconvolution calculations. *J. Chem. Phys.* 76:4419–4432.

Ameloot, M., H. Hendrickx, W. Herreman, H. Pottel, F. van Cauwelaert, and W. van der Meer. 1984. Effect of orientational order on the decay of the fluorescence anisotropy in membrance suspensions: experimental verification on unilamellar vesicles and lipid/α-lactalbumin complexes. *Biophys. J.* 46:525–539.

Busico, V., and M. Vacatello. 1983. Lipid bilayers in the 'fluid' state: computer simulation and comparison with model compounds. *Mol. Cryst. Liq. Cryst.* 97:195–207.

Claesens, F., and R. Rigler. 1986. Conformational dynamics of the anticodon loop in yeast $tRNA^{Phe}$ as sensed by the fluorescence of wybutine. *Eur. Biophys. J.* 13:331–342.

Dale, R. E., L. A. Chen, and L. Brand. 1977. Rotational relaxation of the "microviscosity" probe diphenyl hexatriene in paraffin oil and egg lecithin vesicles. *J. Biol. Chem.* 252:7500–7510.

Dissado, L. A. 1984. The formation of cluster vibrations in imperfectly structured materials. *Chem. Phys.* 91:183–199.

Dissado, L. A., and R. A. Hill. 1982. Dielectric-relaxation and the structure of condensed matter. *Phys. Scr.* T1:110–114.

Dissado, L. A., and R. A. Hill. 1983. A cluster approach to the structure

of imperfect materials and their relaxation spectroscopy. *Proc. R. Soc. Lond. B Biol. Sci.* A390:131–180.

Dissado, L. A., R. R. Nigmatullin, and R. M. Hill. 1985. The fading of memory during the regression of structural fluctuations. *Adv. Chem. Phys.* 63:253–292.

Doniach, S. 1978. Thermodynamic fluctuations in phospholipid bilayers. *J. Chem. Phys.* 68:4912–4916.

Fleming, G. R. 1986. Chemical Applications of Ultrafast Spectroscopy. Oxford University Press, New York.

Fleming, G. R., and A. J. Cross. 1984. Analysis of time-resolved fluorescence anisotropy decays. *Biophys. J.* 46:45–56.

Granville, M. F., G. R. Holtom, and B. E. Kohler. 1980. *Cis-trans* photoisomerization of 1,3,5,7-octatetraene in *n*-hexane at 4.2K. *Proc. Natl. Acad. Sci. USA.* 77:31–33.

Grinvald, A., and I. Steinberg. 1974. On the analysis of fluorescence decay kinetics by the method of least-squares. *Anal. Biochem.* 59:583–598.

Hatta, I., D. Suzuki, and S. Imaizumi. 1983. Pseudo-critical heat capacity of single lipid bilayers. *J. Phys. Soc. Jpn.* 52:2790–2797.

Hatta, I., S. Imaizumi, and Y. Akutsu. 1984. Evidence for weak first-order nature of lipid bilayer phase transition from the analysis of pseudo-critical specific heat. *J. Phys. Soc. Jpn.* 53:882–888.

Heyn, M. P. 1979. Determination of lipid order parameters and rotational correlation times from fluorescence depolarization experiments. *FEBS (Fed. Eur. Biochem. Soc.) Lett.* 108:359–364.

Hudson, B., and S. Cavalier. 1988. Studies of membrane dynamics and lipid-protein interactions with parinaric acid. *In* Spectroscopic Membrane Probes. Vol. 1. L. Loew, editor. CRC Press, Inc., Boca Raton, FL. 43–62.

Hudson, B., D. L. Harris, R. D. Ludescher, A. Ruggiero, A. Cooney-Freed, and S. A. Cavalier. 1986. Fluorescence probe studies of proteins and membranes. *In* Applications of Fluorescence in the Biological Sciences. D. L. Taylor, A. S. Waggoner, F. Lanni, R. F. Murphy, and R. Birge, editors. Alan R. Liss, Inc., New York. 159–202.

Hudson, B., R. D. Ludescher, A. Ruggiero, D. L. Harris, and I. Johnson. 1987. Fluorescence anisotropy decay determinations of rapid reorientational motion: complexities in the interpretation of bilayer acy–chain and protein tryptophan dynamics. *Comments Mol. Cell. Biophys.* 4:171–188.

Hynes, J. T. 1977. Statistical mechanics of molecular motion in dense fluids. *Annu. Rev. Phys. Chem.* 28:301–321.

Hynes, J. T., R. Kapral, and M. Weinberg. 1978. Molecular rotation and reorientation: microscopic and hydrodynamic contributions. *J. Chem. Phys.* 69:2725–2733.

Isenberg, I. 1973. On the theory of fluorescence decay experiments. I. Nonrandom distortions. *J. Chem. Phys.* 59:5696–5707.

Isenberg, I., and R. D. Dysan. 1969. The analysis of fluorescence decay by a method of moments. *Biophys. J.* 9:1337–1350.

Isenberg, I., and E. W. Small. 1982. Exponential depression as a test of estimated decay parameters. *J. Chem. Phys.* 77:2799–2805.

Jahnig, F. 1979*a*. Molecular theory of lipid membrane order. *J. Chem. Phys.* 70:3279–3290.

Jahnig, F. 1979*b*. Structural order of lipids and proteins in membranes: evaluation of fluorescence anisotropy data. *Proc. Natl. Acad. Sci. USA.* 76:6361–6365.

Jahnig, F. 1981*a*. Critical effects from lipid-protein interaction in membranes. I. Theoretical description. *Biophys. J.* 36:329–345.

Jahnig, F. 1981*b*. Critical effects from lipid-protein interaction in membranes. II. Interpretation of experimental results. *Biophys. J.* 36:347–357.

Jahnig, F. 1981*c*. The ordered-fluid transition in lipid bilayers. *Mol. Cryst. Liq. Cryst.* 63:157–170.

Kanehisa, M. I., and T. Y. Tsong. 1978. Cluster model of lipid phase transitions with application to passive permeation of molecules and structure relaxations in lipid bilayers. *J. Am. Chem. Soc.* 100:424–432.

Kawato, S., K. Kinosita, and A. Ikegami. 1977. Dynamic structure of lipid bilayers studied by nanosecond fluorescence techniques. *Biochemistry.* 16:2319–2324.

Kawato, S., K. Kinosita, and A. Ikegami. 1978. Effect of cholesterol on the molecular motion in the hydrocarbon region of lecithin bilayers studied by nanosecond fluorescence techniques. *Biochemistry.* 17:5026–5031.

Kinosita, K., S. Kawato, and A. Ikegami. 1977. A theory of fluorescence depolarization decay in membranes. *Biophys. J.* 20:289–305.

Kinosita, K., A. Ikegami, and S. Kawato. 1982. On the wobbling-in-a-cone analysis of fluorescence anisotropy decay. *Biophys. J.* 37:461–464.

Kowert, B., and D. Kivelson. 1976. ESR linewidths in solution. VIII. Two-component diamagnetic solvents. *J. Chem. Phys.* 64:5206–5217.

Kox, A. J., J. P. J. Michels, and F. W. Wiegel. 1980. Simulation of a lipid monolayer using molecular dynamics. *Nature (Lond).* 287:317–319.

Kremer, J., M. Esker, C. Pathmamanoharan, and P. Wiersema. 1977. Vesicles of variable diameter prepared by a modified injection method. *Biochemistry.* 16:3932–3935.

Lakowicz, J. R. 1983. Principles of fluorescence spectroscopy. Plenum Publishing Corp., New York. 149–163.

Libertini, L., and E. Small. 1983. Resolution of closely spaced fluorescence decays: the luminescence background of the RCA 8850 photomultiplier and other sources of error. *Rev. Sci. Instrum.* 54:1458–1466.

Ludescher, R. D., L. Peting, S. Hudson, and B. Hudson. 1987. The observed decay of fluorescence anisotropy for systems with lifetime and dynamic heterogeneity. *Biophys. Chem.* 28:59–75.

Marquardt, D. W. 1963. An algorithm for least-squares estimation of nonlinear parameters. *J. Soc. Indust. Appl. Math.* 11:431–467.

Mitaku, S., and T. Date. 1982. Anomalies of nanosecond ultrasonic relaxation in the lipid bilayer transition. *Biochim. Biophys. Acta.* 688:411–421.

Mitaku, S., and K. Okano. 1981. Ultrasonic measurements of two-component lipid bilayer suspensions. *Biophys. Chem.* 14:147–158.

Mitaku, S., A. Ikegami, and A. Sakanishi. 1978. Ultrasonic studies of lipid bilayer. Phase transition on synthetic phosphatidylcholine liposomes. *Biophys. Chem.* 8:295–305.

Mitaku, S., T. Jippo, and R. Kataoka. 1983. Thermodynamic properties of the lipid bilayer transition. *Biophys. J.* 42:137–144.

Mouritsen, O., and M. Zuckermann. 1985. Softening of lipid bilayers. *Eur. Biophys. J.* 12:75.

Mouritsen, O., A. Boothroyd, R. Harris, N. Jan, T. Lookman, L. MacDonald, D. Pink, and M. Zuckermann. 1983. Computer simulations of the main gel-fluid transition of lipid bilayers. *J. Chem. Phys.* 79:2027.

Nagle, J. F. 1976. Theory of lipid monolayer and bilayer phase transitions: effect of headgroup interactions. *J. Membr. Biol.* 27:233–250.

Northrup, S. H., and M. S. Curvin. 1985. Molecular dynamics simulation of disorder transitions in lipid monolayers. *J. Phys. Chem.* 89:4707.

Rigler, E. R., and H. E. Ehrenberg. 1973. Molecular interactions and structure as analysed by fluorescence relaxation spectroscopy. *Quant. Rev. Biophys.* 6:139.

Ruggiero, A. J. 1986. Time-resolved fluorescence studies of pretransitional phenomena in phospholipid bilayers. Ph.D. thesis. University of Oregon, Eugene, OR.

Ruggiero, A. J., and B. S. Hudson. 1989. Critical density fluctuations in lipid bilayers detected by fluorescence lifetime heterogeneity. *Biophys. J.* 55:1111–1124.

Sklar, L., B. Hudson, and R. Simoni. 1975. Conjugated polyene fatty acids as membrane probes: preliminary characterization. *Proc. Natl. Acad. Sci. USA.* 72:1649–1653.

Sklar, L., B. Hudson, and R. Simoni. 1976. Conjugated polyene fatty acids as fluorescent membrane probes: model system studies. *J. Supramol. Struct.* 4:449–465.

Sklar, L., B. Hudson, and R. Simoni. 1977*a*. Conjugated polyene fatty acids as fluorescent probes: spectroscopic characterization. *Biochemistry.* 16:813–819.

Sklar, L., B. Hudson, and R. Simoni. 1977*b*. Conjugated polyene fatty acids as fluorescent probes: synthetic phospholipid membrane studies. *Biochemistry.* 16:819–828.

Small, E. W., and I. Isenberg. 1977. On moment index displacement. *J. Chem. Phys.* 66:3347–3351.

Szabo, A. 1984. Theory of fluorescence depolarization in macromolecules and membranes. *J. Chem. Phys.* 81:150–167.

van der Meer, W., H. Pottel, W. Herreman, M. Ameloot, and H. Hendrickx. 1984. Effect of orientational order on the decay of the fluorescence anisotropy in membrane suspensions. *Biophys. J.* 46:515–523.

van der Ploeg, P., and J. C. Berendsen. 1981. Molecular dynamics simulation of a bilayer membrane. *J. Chem. Phys.* 76:3271.

van der Ploeg, P., and J. C. Berendsen. 1983. Molecular dynamics of a bilayer membrane. *Mol. Phys.* 49:233–248.

Wolber, P. K. 1980. A fluorometric study of the structure and acyl chain dynamics of pure phophatidylcholine vesicles, and vesicles containing cholesterol or the M13 coat protein. Ph.D. thesis. Stanford University, Palo Alto, CA.

Wolber, P. K., and B. Hudson. 1981. Fluorescence lifetime and time resolved polarization anisotropy studies of acyl chain order and dynamics in lipid bilayers. *Biochemistry.* 20:2800–2810.

Wolber, P. K. and B. S. Hudson. 1982. Bilayer acyl chain dynamics and lipid-protein interaction. *Biophys. J.* 37:253–262.

Zannoni, C. 1981. A theory of fluorescence depolarization in membranes. *Mol. Phys.* 42:1303–1320.

Zannoni, C., A. Arcioni, and P. Cavatorta. 1983. Fluorescence depolarization in liquid crystals and membrane bilayers. *Chem. Phys. Lipids.* 32:179–250.

Zinsli, P. E. 1977. Anisotropic rotation and libration of perylene in paraffin. *Chem. Phys.* 20:299–309.

Zuckermann, M., and D. Pink. 1980. The correlation length and lateral compressibility of phospholipid bilayers in the presence of thermodynamic density fluctuations. *J. Chem. Phys.* 73:2919–2926.